1995107847

N95-14255

16104

p. 19

Ames Research Center

Comparison of Full-Scale, Small-Scale, and CFD Results for F/A-18 Forebody Slot Blowing

by
Wendy R. Lanser
Larry A. Meyn
NASA Ames Research Center
Moffett Field, CA

Kevin D. James
Sterling Federal Systems, Inc.
Moffett Field, CA

1994 High Alpha Conference July 12-14, 1994

Abstract

It has been shown experimentally that pneumatic forebody flow control devices provide a significant increase in yaw control for fighter aircraft at high angle-of-attack. This study presents comparisons of the various experimental and computational results for tangential slot blowing on the F/A-18 configuration. Experimental results are from the full-scale and 6%-scale model tests and computational solutions are from both isolated forebody and full aircraft configurations. The emphasis is on identifying trends in the variation of yawing moment with blowing-slot exit conditions. None of the traditional parameters (mass flow ratio, blowing momentum coefficient, velocity ratio) succeeded in collapsing all of the results to a common curve. Several factors may affect the agreement between the 6%- and full-scale results including Reynolds number effects, sensitivity of boundary layer transition from laminar to turbulent flow, and poor geometric fidelity, particularly of the blowing slot. The disagreement between the full-scale and computed yawing moments may be due to a mismatch in the slot exit conditions for the same mass flow ratio or aircraft configuration modeling. The general behavior of slot blowing on the 6%-scale and computational models is correct, but neither match the full-scale results.

— Ames Research Center — **Objectives**

F/A-18 Forebody Slot Blowing

- **Correlations of Full-Scale and 6%-Scale Results**
  - non-dimenstional parameters
  - scale effects
  - performance
- **Comparisons of Computations and Experiments**
  - performance
  - surface pressures

Introduction

Wind tunnel testing has been and continues to be the best way to obtain accurate estimates of the aerodynamic performance of a vehicle before building a prototype. For many applications, small-scale model testing is appropriate and sufficient. In some cases, for example when model fidelity is critical or significant amounts of flow separation are present, results may be sensitive to Reynolds number, and large-scale testing is in order. Along with wind-tunnel testing, computational fluid dynamic (CFD) solutions are a useful tool in generating estimates of aerodynamic performance before a prototype is built.

It has been shown experimentally that pneumatic forebody flow control devices provide a significant increase in yaw control for fighter aircraft at high angles-of-attack. This control capability has been demonstrated in small-scale and full-scale experiments as well as in computational solutions using Navier Stokes equations. This study presents comparisons of the various experimental and computational results for tangential slot blowing on the F/A-18 configuration. Experimental results are from full-scale and 6%-scale model tests and the computational results are from both the isolated forebody and the full aircraft configurations. The full-scale experiment was conducted in the 80- by 120-Foot Wind Tunnel, the 6%-scale model was tested in the 7- by 10-Foot Wind Tunnel, and the computations performed at the Numerical Aerodynamic Simulation Facility at NASA Ames Research Center. The emphasis is on identifying trends in the variation of yawing moment with blowing-slot exit conditions. Definition of an appropriate non-dimensional slot-exit parameter may allow direct comparisons of the CFD and the small-scale experimental results with the full-scale experimental results. The traditional non-dimensional parameters: mass flow ratio, blowing momentum coefficient, and velocity ratio will be evaluated in an attempt to collapse all of the results to a common curve. Additionally, the comparison of experimental and computed surface pressure distributions will be presented. The test conditions included variation in angle-of-attack from 25 to 60 deg, and free-stream velocities from 95 to 157 ft/sec for the 6%-scale model and 40 to 168 ft/sec for the full-scale model. The Reynolds number based on wing mean aerodynamic chord ranged from 0.387×10^6 to 0.636×10^6 for the 6%-scale model, from 4.5×10^6 to 12.0×10^6 for the full-scale aircraft, and 11×10^6 for the computational solutions.

Ames Research Center

Model Descriptions

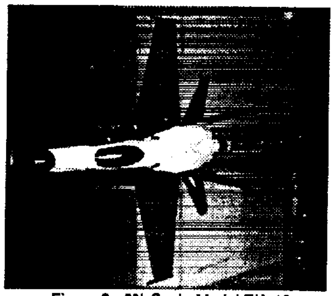

Figure 2. 6% Scale-Model F/A-18

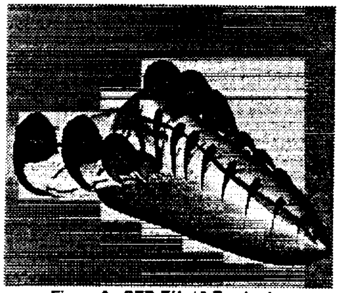

Figure 3. CFD F/A-18 Forebody

Figure 1. Full-Scale F/A-18

1994 High Alpha Conference July 12-14, 1994

Model Descriptions

<u>Full-scale Aircraft</u>

The full-scale F/A-18 aircraft tested was a single-seat aircraft built by the McDonnell Douglas Aircraft and the Northrop corporations. The F/A-18 fighter aircraft has two vertical stabilizers canted 20 deg outboard from the vertical and has leading edge extensions (LEXs) on each side of the fuselage just forward of the wing. The LEXs used for this experiment were instrumented for surface pressures and were flown on the High Alpha Research Vehicle at the Dryden Flight Research Facility in 1990, reference 1. During the wind-tunnel test, the aircraft had both engines removed, air flow through the engine inlets, the wingtip missile launch racks mounted, and the control surfaces configured for high-angle-of-attack flight. The high angle-of-attack configuration has the leading-edge flaps set at 33 deg and the trailing-edge flaps set at 0 deg. The horizontal tails operated on a flight control schedule that was a function of the angle-of-attack to simulate trimmed flight conditions. The rudders were positioned at 0 deg deflection unless noted otherwise.

The radome designed for these experiments incorporated a variable-length slot, pneumatic forebody-flow-control mechanism interior to the radome structure. This radome was a composite laminate of fiberglass/foam/fiberglass fabricated from a plastic mold formed on a production-aircraft radome. Figure 1 above shows the slot highlighted with a white stripe on the radome; only the port slot was active. Care was taken to assure symmetry by incorporating a dummy slot on the starboard side.

The blowing slot had a total length of 48 inches and began 3 inches aft of the radome apex. The slots were positioned at 90 deg and 270 deg from the windward side (bottom) of the radome. The active slot was at the 270 deg position (port-side) and was designed to blow tangentially to the surface toward the leeward side of the radome. The 48 inch slot was divided into 24 separately controlled segments with each segment measuring 2 inches long. The slot height was 0.10 inches. Air for the slot was supplied by several 125 psi compressors, totaling 1550 CFM. The mass flow rate of the blowing air was measured using a turbine flow meter.

A three-strut configuration was used to mount the F/A-18 aircraft in the 80-by 120-Foot Wind Tunnel test section. The aircraft was attached to a circular cross beam at the two main landing gear positions, which in turn was attached to the wind-tunnel main struts. A tail boom assembly, connected to the aircraft at each engine mounting pin and at the arresting tail hook hard point, was used to attach the aircraft to the third wind-tunnel tail strut. The angle-of-attack was varied by altering the length of the tail strut. The angle-of-attack range for the full-scale forebody flow control experiment was from 20 to 50 deg. Additional details can be found in references 2-4.

6%-scale Model

The 6% model (fig. 2) for this experiment was a new model designed and built by Eidetics International. A fiberglass model was made from a mold made from a Navy/McAir 6% model. During the wind tunnel test, the engine inlet was faired over, the leading-edge flaps were deflected 34 deg, the trailing edge flaps at 0 deg, the horizontal tails fixed at 0 deg, and the rudders were positioned at 0 deg deflection unless otherwise noted.

The radome on this model had blowing slots on both sides made up of four segments. The slot had a total length of 1.92 inches, a width of 0.006 inches, and began 0.66 inches aft of the radome apex. This slot configuration corresponded to a 32 inch long slot located 11 inches aft of the radome apex at full-scale. The slots were positioned at 90 deg and 270 deg from the windward side (bottom) of the radome. Various slot lengths were tested by taping over portions of the slot segments. The interior of the nose contained two plenums, one on the starboard side and one on the port side that supplied air to the blowing slots. The mass flow rate of the blowing air was measured with an Omega volumetric flow meter. The volumetric flow meter was calibrated using an extremely sensitive (0.1 gram) scale and a regulated supply tank.

The 6%-scale model was sting mounted with the wings vertical, and the model was pitched in the horizontal direction with the floor mounted turntable. The angle-of-attack range for this experiment varied from 20 to 60 deg. Further details of this experiment can be found in reference 5.

Computational Analysis

The computational results presented here for the yawing moment coefficient as a function of blowing rate are for both the isolated forebody (fig. 3) and the full aircraft geometry. The computed pressure distributions presented are for the full aircraft geometry only. The aircraft and slot geometry were modeled using an overset grid technique, references 6-8. The full computational aircraft geometry had a faired-over engine inlet. The computational slot geometry is identical to the geometry used in the full-scale wind tunnel test. For both of these computations, a three-dimensional, thin-layer, implicit Navier-Stokes code with the Degani-Schiff modified Baldwin-Lomax algebraic turbulence model was used, references 6-8. The solutions for the forebody blowing conditions were computed at 30 deg angle-of-attack.

Ames Research Center

Experiment Description

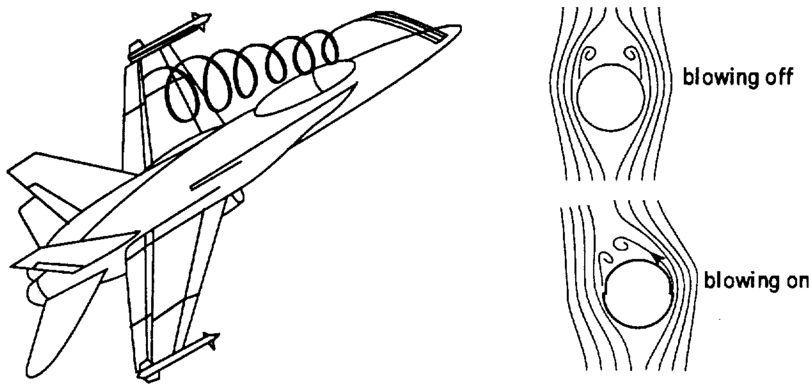

Mass Flow Ratio $= MFR = \dot{m}_{slot}/\rho_\infty U_\infty S_{wing}$

Blowing Momentum Coefficient $= C\mu = \dot{m}_{slot} U_{slot}/q_\infty S_{wing}$

Velocity Ratio $= U_{slot}/U_\infty$

1994 High Alpha Conference July 12-14, 1994

Experiment Description

These experiments measured the forces and moments on the aircraft due to the tangentially blowing slot. The tangentially blowing slot concept is based on the flow phenomenon called the coanda effect. The coanda effect delays the flow separation over a curved surface. This phenomenon creates a low pressure on the blowing side of the radome resulting in a suction force. The results presented show the yawing moment generated by the slot blowing for several slot configurations. In some cases the effect of the tangentially blowing slot was evaluated as the difference between the blowing-off and blowing-on conditions, ΔCn.

In the full-scale experiment, the yawing moment was measured using the external wind-tunnel balance system. During the 6%-scale wind tunnel test, the yawing moment was measured with an internal sting-mounted six-component balance. The moment reference was located at the 25% mean aerodynamic chord for both experiments and the CFD analyses.

Data from the full-scale wind-tunnel test have been corrected for blockage effects using techniques described in reference 9. The correction for blockage varied with the angle-of-attack. For example, at 50 deg angle-of-attack and q_∞ of 33 psf, the dynamic pressure had a correction of 3.8%, and a measured pressure coefficient of -1.0 at 30 deg angle-of-attack had a correction of 0.058.

In order to compare results from the 6%-scale test, the full-scale test, and the computational solutions non-dimensional slot exit parameters are required. As a result, the 6%-scale and the full-scale tests measured the blowing mass flow rate to determine the mass flow ratio, MFR. MFR is defined as the ratio of the mass flow rate through the slot to a reference mass flow rate. The reference mass flow rate is based on free-stream density, velocity, and the wing reference area. For both the full-scale and 6%-scale tests measured mass-flow rate, slot-exit area, and wind-tunnel static pressure were used to determine the slot exit conditions. In the full-scale test the total temperature in the plenum was used to determine slot exit conditions while the wind-tunnel total temperature was used in the 6%-scale test. Based on these measurements, the exit Mach number, the velocity, and the blowing momentum coefficient were determined using the continuity relationships for compressible flow defined in reference 10. This relationship assumed a uniform exit velocity and slot exit area.

To better understand the influence of the pneumatic forebody flow control on the flow-field structure, time-averaged pressures were measured on the forebody. The pressure orifices were located at five fuselage stations (FS): three circumferential rings on the radome at FS 70, 85, and 107, and two circumferential rings on the forebody at FS 142 and 184. The radome apex was located at FS 60.5, and the fuselage stations were measured in inches from that point.

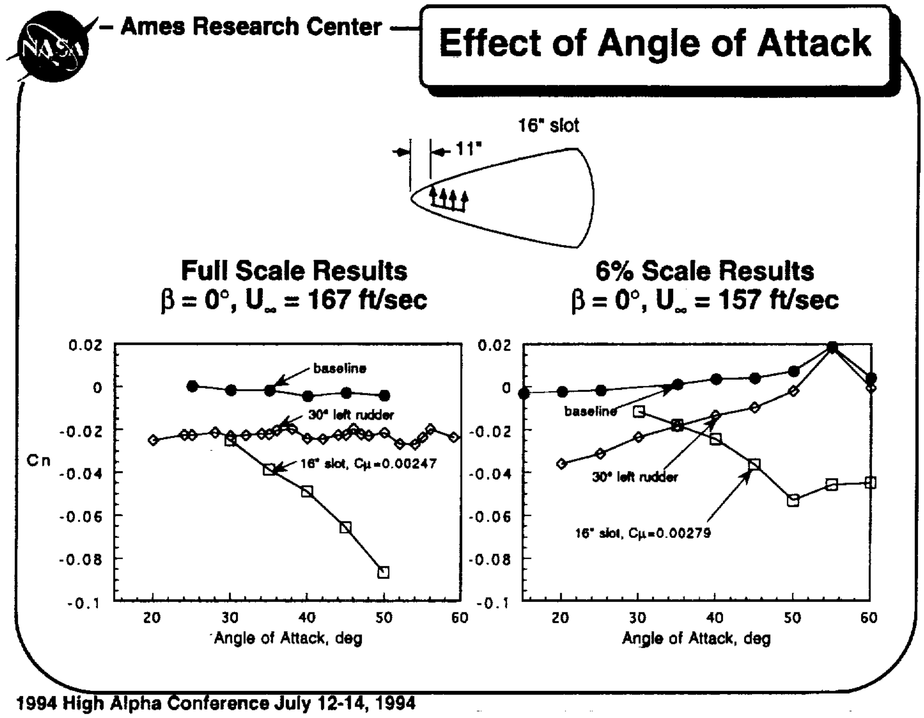

Results: Effect of Angle-of-Attack

The figure above shows the yawing moments generated by the baseline, no blowing, configuration, 30 deg of left rudder deflection, and blowing through a 16 inch slot located 11 inches aft of the radome apex for full-scale experiment and the corresponding configuration for 6%-scale experiment (0.96 inch slot located 0.66 inches aft). These results show that for a similar blowing momentum coefficient, $C\mu$, the small-scale model is less effective than the full-scale model. Also of interest, the small-scale results show an asymmetry above 50 deg angle-of-attack. Additionally, the rudder effectiveness decreased as angle-of-attack increased, which has been seen in other small-scale tests. However, the full-scale experiment shows the rudder effectiveness to be nearly constant across the angle-of-attack range from 20 to 60 deg. At 35 deg angle-of-attack, nearly the same magnitude of yawing moment was generated due to the rudder deflection at full-scale as was generated in the small-scale experiment. One noted difference was that the 6%-scale model had the horizontal tail fixed at 0 deg, and the full-scale experiment operated the horizontal tails on a flight control schedule that was a function of the angle-of-attack to maintain trimmed flight conditions. During the full-scale experiment, the 30 deg rudder case was re-run with the horizontal tails fixed at 0 deg and the same trend in the yawing moment was observed. As previously mentioned, the full-scale blowing experiment was limited to 50 deg angle-of-attack. The additional 30 deg rudder deflection data from 50 to 60 deg angle-of-attack was obtained during a second full-scale wind tunnel entry.

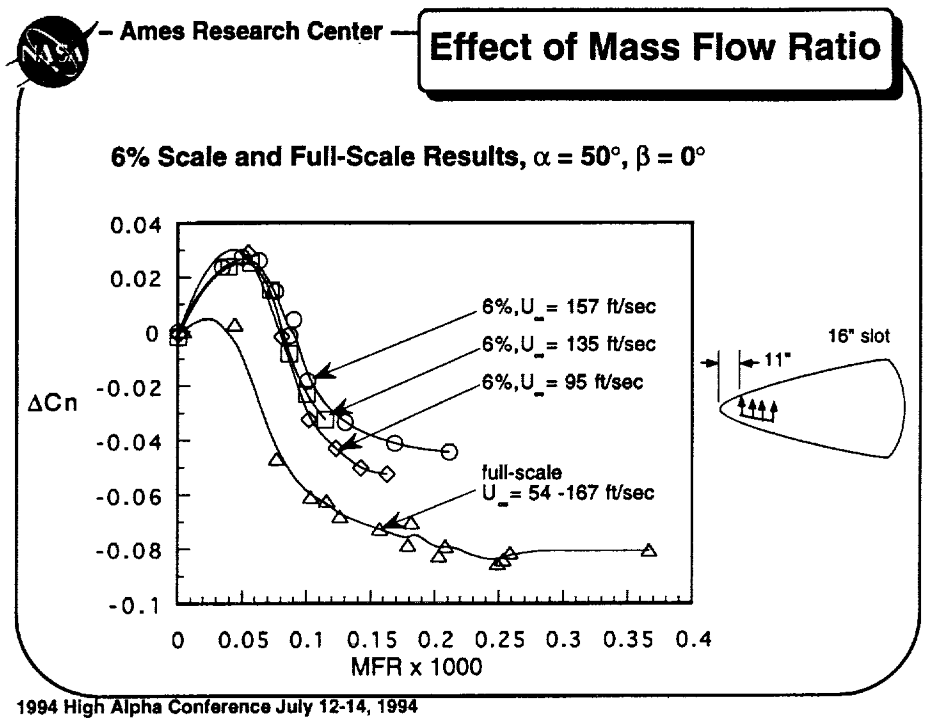

Results: Effect of Mass Flow Ratio

The results shown above are for the 16 inch long slot positioned 11 inches aft of the radome apex for the full-scale experiment and the corresponding 6%-scale configuration (0.96 inches long 0.66 inches aft). The figure above shows the yawing moment generated by the slot blowing as a function of the mass flow ratio (MFR) at 50 deg angle-of-attack. The 6%-scale data show a less effective slot than the full-scale slot for the same MFR. The full-scale data collapses fairly well to a single curve for the MFR range investigated, which included a free-stream velocity range from 40 ft/sec to 167 ft/sec. Whereas, the 6%-scale slot does not collapse the data to a single curve for the free-stream velocity range tested. The small-scale data also show an amplified moment reversal at low blowing rates when compared to the full-scale results. A few possible explanations for the differences found between the two sets of results are forebody geometry fidelity, surface roughness, and Reynolds number effect. Any one of these explanations or a combination of them may cause the flow in the boundary layer on the forebody region of the aircraft to transition from laminar to turbulent differently from the small-scale test to the large-scale test and more importantly to separate at different points on the forebody.

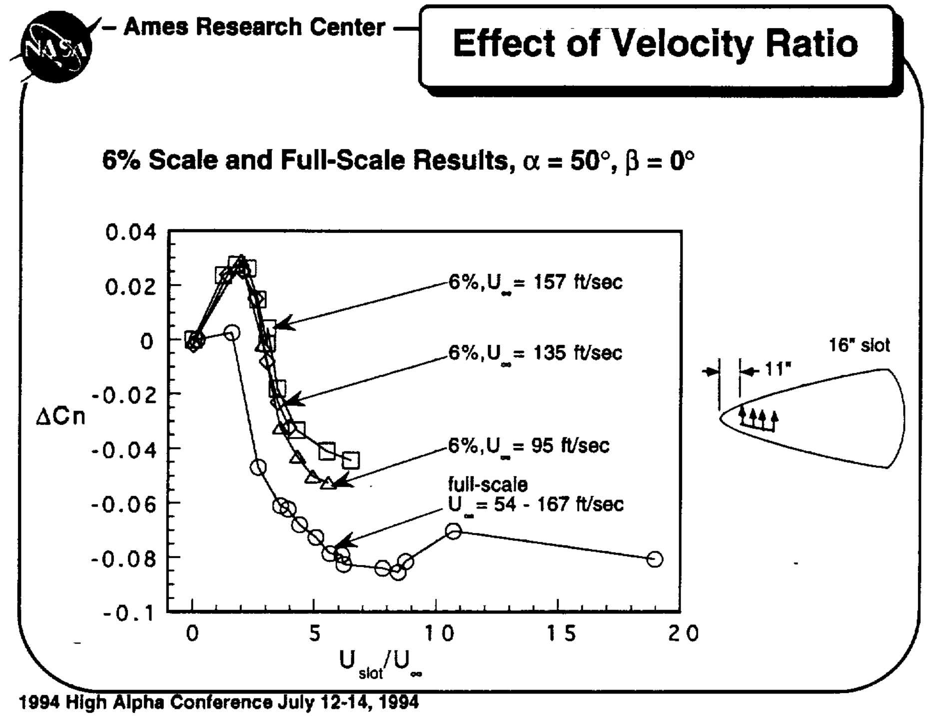

Results: Effect of Velocity Ratio

The yawing moment generated by the slot blowing for the same slot configurations and angle-of-attack are shown above as a function of the velocity ratio. The velocity ratio is defined as the ratio of the slot exit velocity to the free-stream velocity. The data from the 6%-scale model test appear to collapse slightly better as a function of the velocity ratio than when plotted as a function of the MFR. Similar to the previous comparison using MFR to non-dimensionalize the blowing slot-exit conditions, the small-scale test produced less yawing moment than the full-scale test for the same velocity ratio and showed an amplified moment reversal at the low blowing rates.

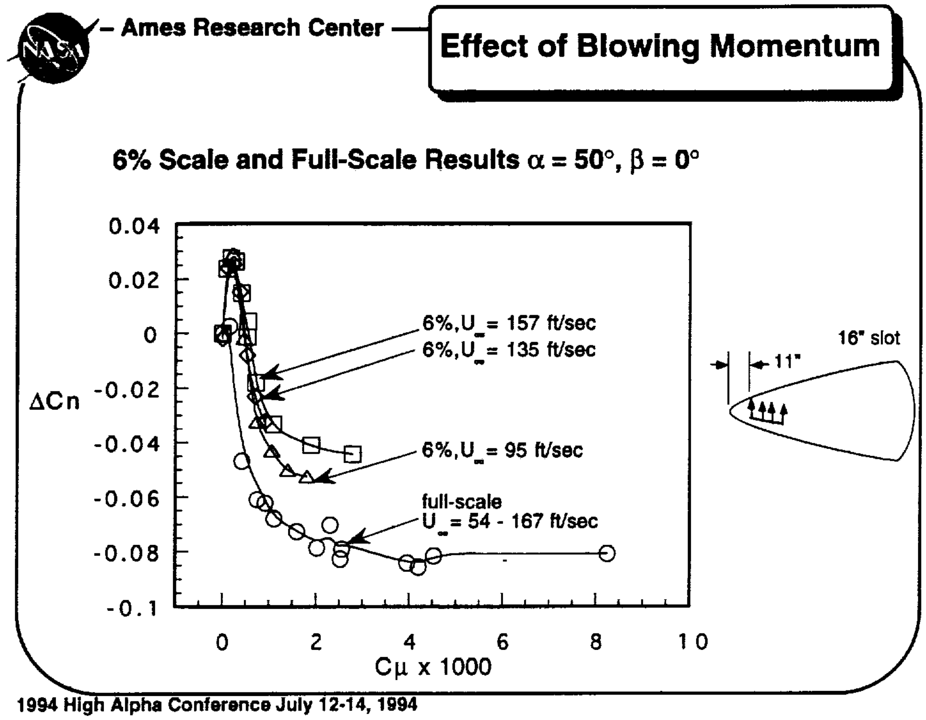

Results: Effect of Blowing Momentum Coefficient

Again for the 16 inch slot positioned 11 inches aft of the radome apex for the full-scale configuration and the corresponding 6%-scale model configuration, the yawing moment due to slot blowing is shown as a function of the blowing momentum coefficient. The blowing momentum coefficient, $C\mu$, is a velocity squared function as defined in the experiment description figure. The full-scale results collapse to a common curve better as a function of the $C\mu$ than as a function of the velocity ratio. The 6%-scale data appears to collapse slightly better at the lower blowing rates as a function of $C\mu$ than as function of velocity ratio; however, at higher blowing rates the velocity ratio parameter appears slightly better than the $C\mu$ parameter. The comparison of the yawing moments as a function of $C\mu$ for the small-scale with the full-scale yields similar results to those seen for the MFR and velocity ratio parameters.

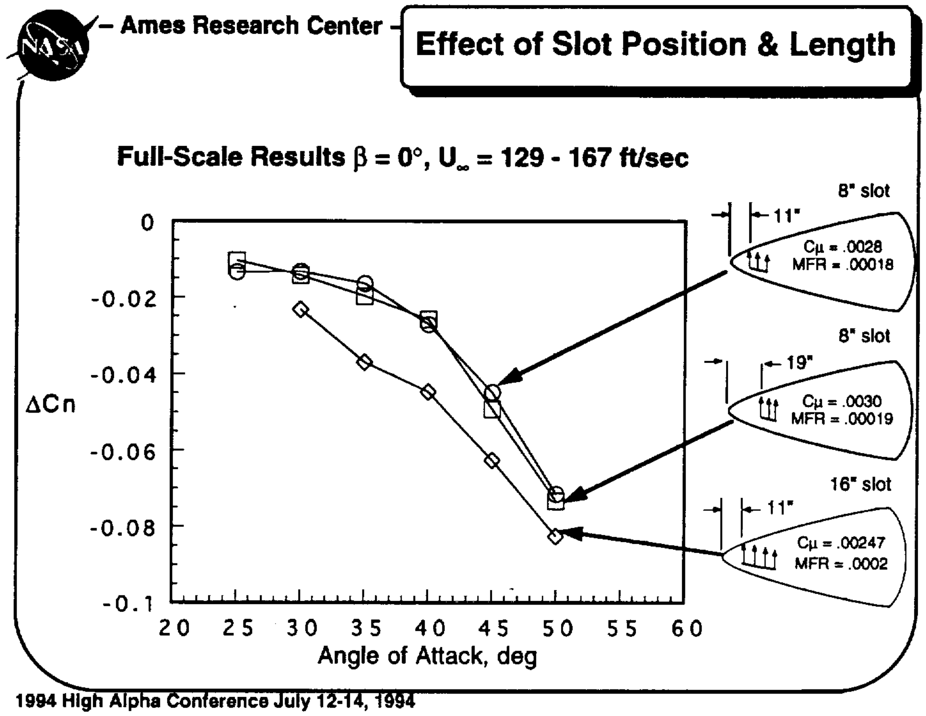

Results: Effect of Slot Position and Length for the Full-scale Results

In the figure above, the yawing moment generated by three full-scale slot configurations for similar Cμ values over an angle-of-attack range from 20 to 50 deg are shown. The slot configurations shown are the 8 inch long 11 inches aft, 8 inch long 19 inches aft, and 16 inch long 11 inches aft. The position of the slot relative to the radome apex had no effect on the 8 inch slot configurations. However, the 16 inch long slot positioned 11 inches aft produced more yawing moment than either one of the 8 inch long slot configurations for a lower Cμ value. Even though the MFR did not change in going from the 8 inch slot to the 16 inch slot, the yawing moment increased significantly.

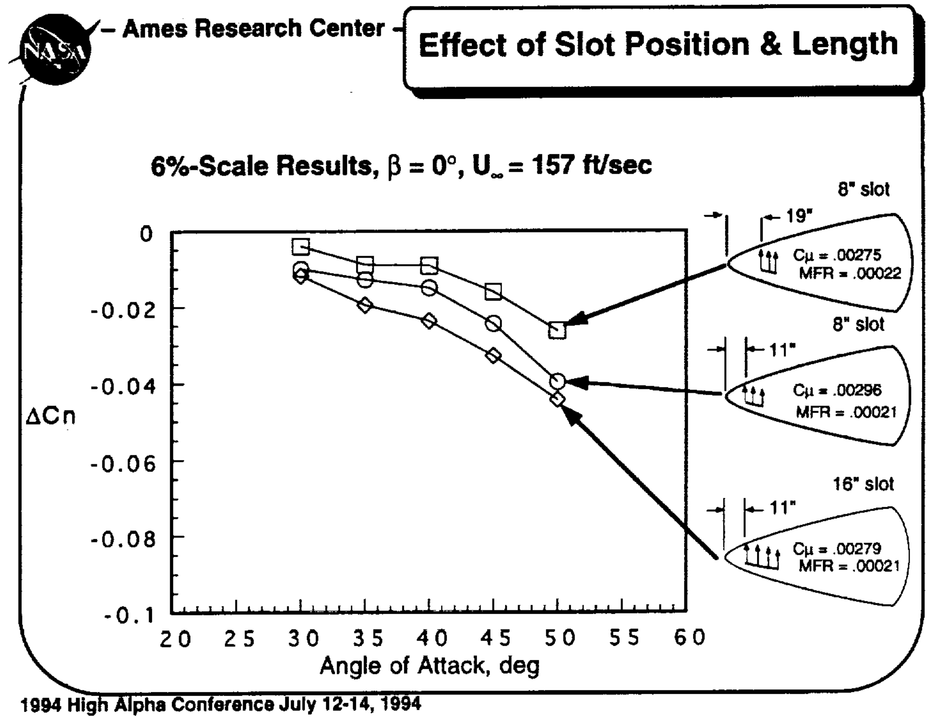

Results: Effect of Slot Position for the Small-scale Results

Shown above are the yawing moments generated by the the three 6%-scale model configurations that correspond to the three full-scale configurations shown on the previous page for similar Cμ values over the angle-of-attack range from 20 to 50 deg. Again, the slot configurations shown are the 0.48 inches 0.66 inches aft (8 inch long 11 inches aft full-scale) , 0.48 inches 1.14 inches aft (8 inch long 19 inches aft full-scale), and 0.96 inches 0.66 inches aft (16 inch long 11 inches aft full-scale). In contrast to the full-scale experiment, the 6%-scale model showed an effect of the slot position relative to the radome apex on the amount of yawing moment generated. The discrepancy shown between the 6%-scale model configurations of the 8 inch slots combined with test notes indicating poor flow quality from the forward slot position suggest that there was non-uniform flow at the slot exit. These results for the 8 inch slots could also indicate that the location of the boundary layer transition from laminar to turbulent flow differ on the 6%-scale model than on the full-scale model. Similar to full-scale results, the 6%-scale model of the 16 inch slot positioned 11 inches aft produced more yawing moment than both the 8 inch slots.

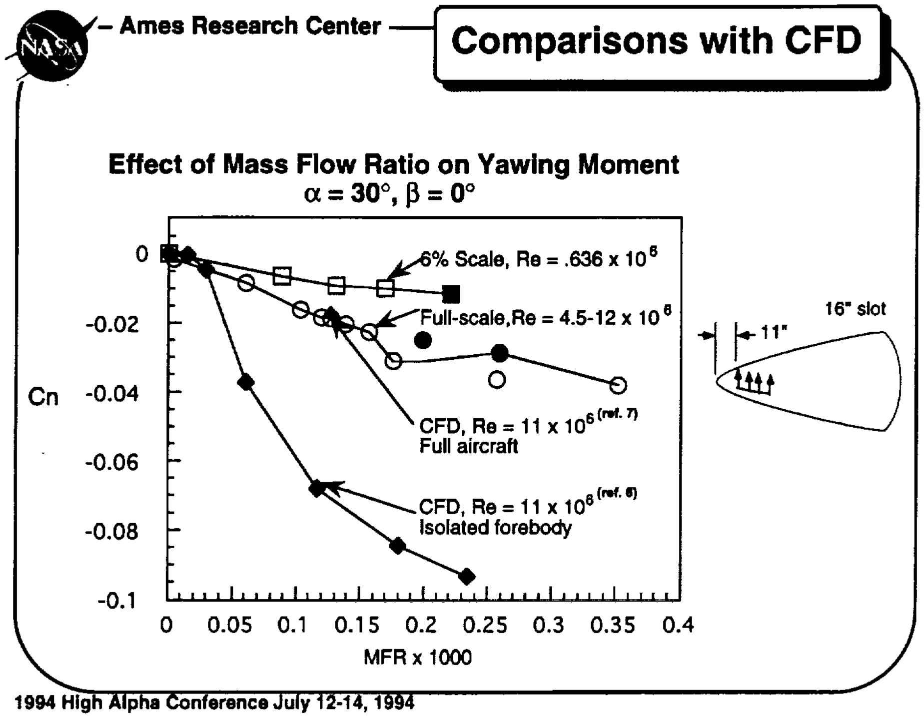

Results: Comparison of Small-scale, Full-scale, and CFD Results

The figure above shows the yawing moment as a function of MFR for the 16 inch slot positioned 11 inches aft at 30 deg angle-of-attack for both the small-scale and full-scale wind tunnel tests, as well as computational solution for the isolated forebody and full aircraft-configuration. In the figure above, the data points shown in black indicate that the exit velocity conditions were sonic. As seen in previous comparisons of the small-scale to full-scale results, the small-scale tests produced smaller yawing moments than the full-scale tests did at the same mass flow ratio. The computational analyses for the isolated forebody significantly over predicted the yawing moment produced in either one of the experiments. However, the computational analyses for the full-aircraft configuration yields a time-accurate solution that falls on the curve with the full-scale experimental results. It is important to note that for the isolated forebody and full-aircraft configuration computational solutions there was a mismatch in both the slot exit conditions and the free-stream Mach numbers. The maximum Mach number for the full-scale experiment was 0.15 whereas the computed solutions had a free-stream Mach number of 0.243. These computational solutions suggest that while the full-aircraft may not be critical for qualitatively capturing the global flow physics it is critical for accurate predictions of force magnitudes and blowing strengths.

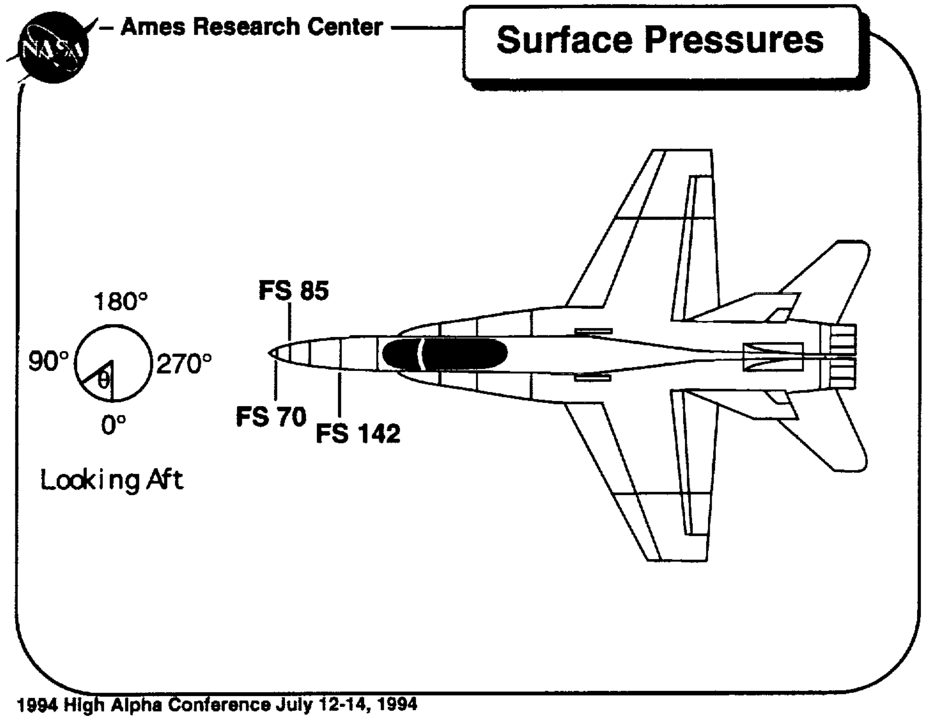

Forebody Fuselage Stations

As previously mentioned, time-averaged pressures were measured on the forebody to better understand the flow-field. Pressure orifices were located at five fuselage stations (FS): three circumferential rings on the radome at FS 70, 85, and 107, and two circumferential rings on the forebody at FS 142 and 184 for the full-scale model and the corresponding FS on the 6%-scale model. The radome apex was located at FS 60.5, and the fuselage stations were measured in inches from that point. Pressure distributions will be shown at FS 70, 85, and 142.

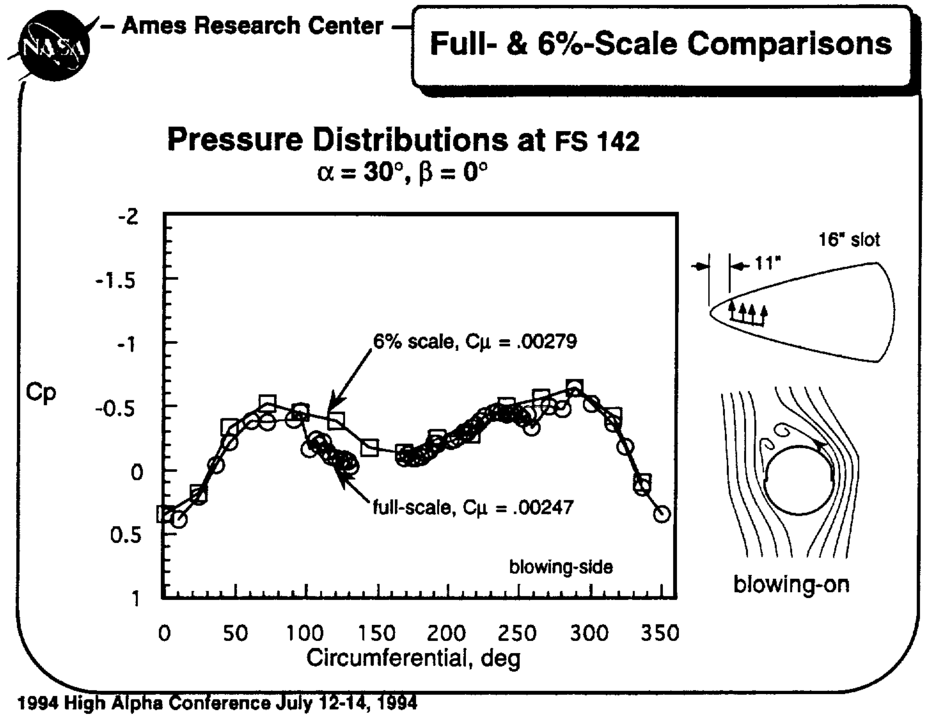

Results: Full-scale and 6%-Scale Pressure Distribution Comparisons

The figure above shows the pressure distributions for FS 142 on the aircraft at 30 deg angle-of-attack for both wind tunnel experiments at similar slot-blowing conditions. Agreement of data was within a reasonable range. As was expected, there is a decrease in pressure on the blowing side of the radome and an increase in pressure on the non-blowing side of the radome. The full-scale experiment showed a higher pressure on the non-blowing side of the radome. This result supports the larger forces seen in the full-scale data for the yawing moment comparisons. The discontinuities in the full-scale data at circumferential angles of approximately 95 deg and 265 deg are due to an antenna fairing which protrudes just forward of the orifice. Also, pressure taps could not be located between the circumferential angles of 131 deg and 167 deg due to structural obstructions inside the aircraft.

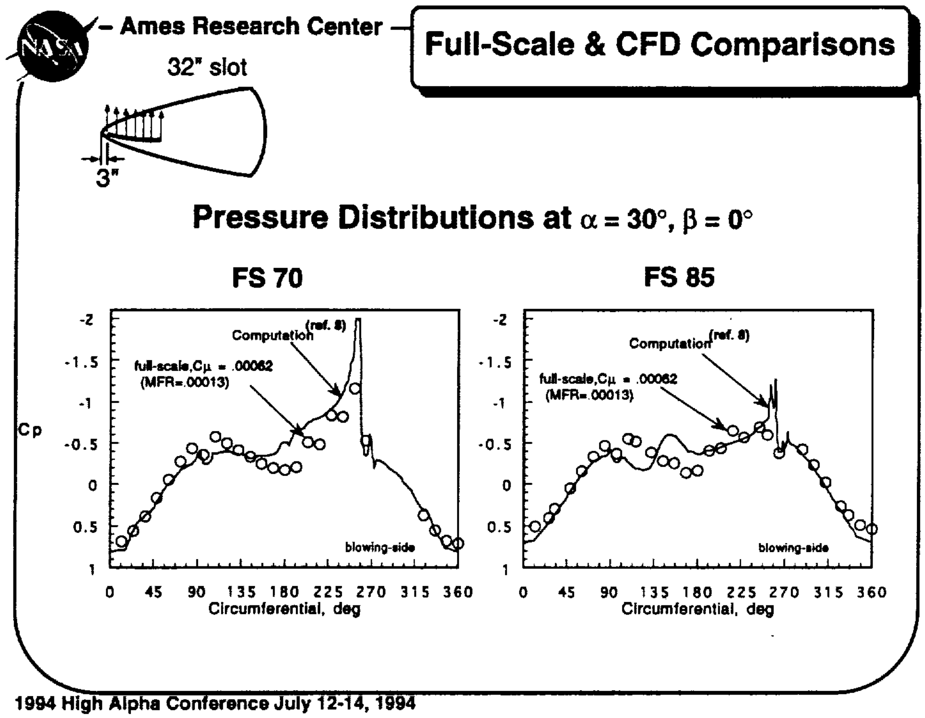

Results: Full-scale and CFD Pressure Distribution Comparisons

For the 30 deg angle-of-attack condition and the 32 inch long slot position 3 inches aft, the pressure distributions are shown for FS 70 and FS 85. The computed pressures are for the full-aircraft configuration, reference 8. Reasonable agreement is shown: the essential flow characteristics seen in the wind tunnel are captured in the computed solution. For these datasets, there is closer agreement in pressure distributions between the full-scale measurements and the computational solution on the leeward side than on the windward side of the radome.

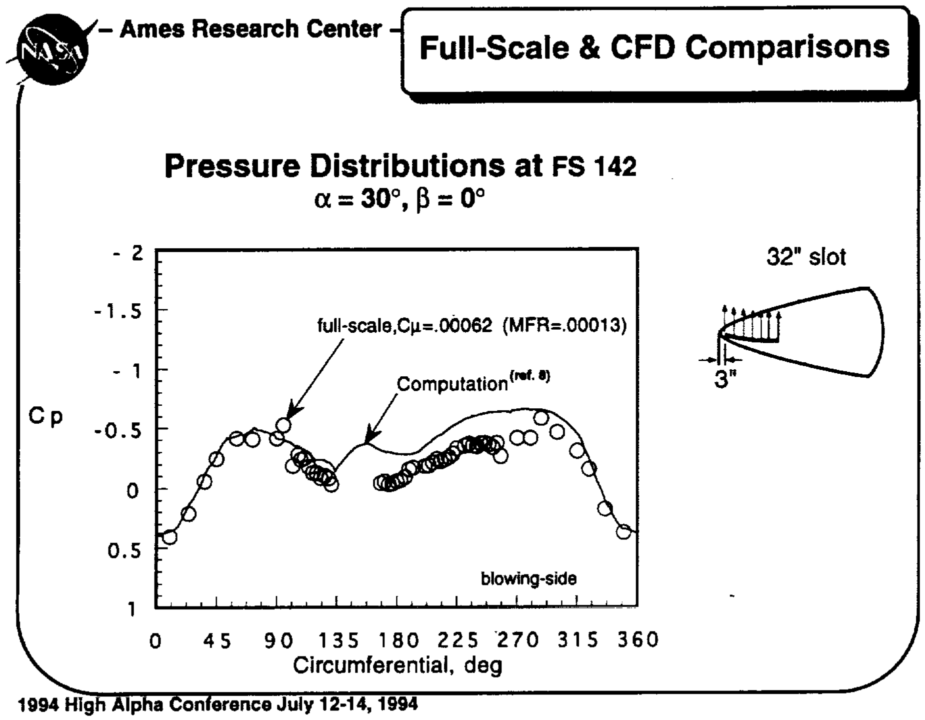

Results: Full-scale and CFD Pressure Distribution Comparisons

The data above shows pressure distributions at FS 142 on the aircraft for the 32 inch slot positioned 3 inches aft of the radome apex at 30 deg angle-of-attack. The computed solution includes the full-aircraft geometry. While the correspondence in the data between the computed solution and the full-scale wind tunnel measurements is promising, there are some differences in the magnitudes. As noted previously, the discontinuities in the full-scale data at circumferential angles of approximately 95 deg and 265 deg are due to an antenna fairing which protrudes just forward of the orifice, and the gap in the data between circumferential angles of 131 deg and 167 deg due to structural obstructions inside the aircraft.

Ames Research Center

Summary

- **6%-Scale Effective Tool**
  - proof of concept
  - ID appropriate non-dimensional parameters
- **Computational Solutions Effective Tool**
  - proof of concept
  - predicted trends but lacking fidelity
- **Large Scale Testing Required to**
  - capture important scale effects
  - measure aerodynamic performance
  - obtain detailed aerodynamic data base

1994 High Alpha Conference July 12-14, 1994

Summary

This study presented comparisons of the various experimental and computational results for tangential slot blowing on the F/A-18 configuration. Experimental results are from full-scale and 6%-scale model tests and the computational results are for both the isolated forebody and full aircraft configurations. The emphasis was on identifying trends in the variation of yawing moment with slot-exit conditions. None of the traditional parameters (mass flow ratio, blowing momentum coefficient, velocity ratio) succeeded in collapsing all of the results to a common curve. For the conditions investigated, the 6%-scale tangential slot blowing experiment generated smaller yawing moments than the full-scale experiment, as well as showing an amplified moment reversal at the low blowing rates. Several factors may affect the agreement between the 6%- and full-scale results including Reynolds number effects, sensitivity of boundary layer transition from laminar to turbulent flow, and poor geometric fidelity particularly of the blowing slot. More detailed data are required to identify the cause of the disagreement between these two experiments.

The comparisons of the computational solutions with the full-scale experiment show some interesting results. The computations with the isolated forebody significantly over predicted the yawing moment generated for the slot blowing and the blowing strength required, but the full-aircraft configuration yielded a time-accurate solution that matched the full-scale experimental results. Another important point in these comparisons was that the slot-exit conditions and free-stream Mach number did not match. The disagreement between the full-scale and CFD yawing moments, particularly for the isolated forebody, may be due to a mismatch in the slot exit conditions for the same mass flow ratio or aircraft configuration modeling.

The general behavior of slot blowing on the 6%-scale and computational models is correct, but neither match the full-scale results. It appears that modeling of this flow field requires greater fidelity than currently feasible for both the small-scale test and CFD.

References

1. Fisher, D., Banks, D., and Richwine, D. M., "F-18 High Alpha Research Vehicle Surface Pressures: Initial In-Flight Results and Correlation With Flow Visualization and Wind-Tunnel Data," AIAA Paper 90-3018, Aug. 1990.
2. Lanser, W. R. and Meyn, L. A., "Forebody Flow Control on a Full-Scale F/A-18 Aircraft," AIAA Paper 92-2674, June 1992.
3. Meyn, L. A., Lanser, W. R., and James, K. D., "Full Scale High Angle of Attack Tests of an F/A-18," AIAA Paper 92-2676, June 1992.
4. Lanser, W. R., "Wind Tunnel Measurements on a Full-Scale F/A-18 With a Tangentially Blowing Slot," NASA CP-10134, Feb. 1994.
5. Kramer, B. R., Suarez, C., Malcolm, G., and Ayers, B.F., "F/A-18 Forebody Vortex Control Volume 1 - Static Tests," NASA CR 4582, March 1994.
6. Gee, K. and Rizk, Y. M., "Analysis of Tangential Slot Blowing on F/A-18 Isolated Forebody," AIAA Paper 94-1831, Jan. 1994.
7. Gee, K. and Rizk, Y. M., "Effect of Forebody Tangential Slot Blowing on Flow About a Full Aircraft Geometry," AIAA Paper 93-2962, July. 1993.
8. Gee, K. and Rizk, Y. M., "Analysis of of a Pneumatic Forebody Flow Control Concept About a Full Aircraft Geometry," AIAA Paper 92-2678, June. 1992.
9. Rae, W. H. Jr, and Pope, A., Low Speed Wind Tunnel Testing, Second Edition, 1984.
10. Society of Automotive Engineers, Inc., "Thermodynamics of Incompressible and Compressible Fluid Flow," AIR1168/1, Mar. 1990, pp. 85-87.